

Taking into account inhomogeneous distortion around the pressuremeter probe to determine shear modulus

Julien Habert

Terrasol, Paris, France, julien.habert@setec.com

Sébastien Burlon

Terrasol, Paris, France, sebastien.burlon@setec.com

ABSTRACT: Pressuremeter test constitutes an efficient tool to determine stiffness of the ground, and especially shear modulus of ground, and its reduction with the distortion level. However, the inhomogeneous distortion level around a pressure meter probe, reducing with the radial distance to the probe, and subsequent inhomogeneous value of the shear modulus, have to be taken into account to correctly interpret pressuremeter test results.

On a first step, based on currently used shear modulus reduction hyperbolic curves to link distortion and shear modulus, the evolving of these parameters around a pressuremeter probe, is presented for different stress levels in the case of a purely cohesive soil. On a second step, a practical procedure is proposed to derive distortion-shear modulus from a pressuremeter test. On a third and last step, the proposed method is applied to a test performed in purely cohesive soil.

Keywords: pressuremeter ; shear modulus ; distortion ; nonlinear elasticity

1. Introduction

Pressuremeter test constitutes an efficient tool to determine stiffness of the ground, and especially shear modulus of ground, and its reduction with the distortion level.

For purely cohesive soils closed form solution have been developed for the relation between applied pressure and volume of the pressuremeter probe, first by Gibson and Anderson (1961, [9]), in considering a linear elastic behaviour. Later on, Jefferies (1988, [10]) developed the previous relationship also for unloading part of the test. These first approaches provided an efficient tool to analyse pressuremeter tests but appeared not consistent with constitutive law allowing a degradation of shear modulus with distortion (or shear strain) level. Ferreira and Robertson (1992, [5]) first proposed to derive pressuremeter expansion curve in using a hyperbolic degradation law for distortion-secant shear modulus relationship. Bolton and Whittle (1999, [2]) choose distinct hyperbolic law.

The present article proposes to use a nonlinear elastic current constitutive law similar to the one chosen by Ferreira and Robertson (1992, [5]), but with a different implementation approach: it then allows to recover and confirm their results but also to have access to the stress state, especially distortion level and actualized shear modulus at difference distances of the pressuremeter probe. It also provides practical tips to derive shear modulus from the pressuremeter test.

2. Proposed Approach

2.1. Hypothesis

2.1.1. Basic equations

Under plane strain analysis, equilibrium fulfills Equation (1).

$$r \frac{d\sigma_r}{dr} + (\sigma_r - \sigma_\theta) = 0 \quad (1)$$

where σ_r and σ_θ are respectively the radial and orthoradial stresses, and r the actual radial distance from the axis pressuremeter probe, evolving throughout the test, as given in Figure 1.

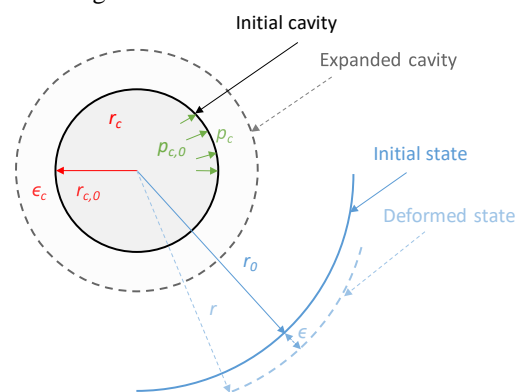


Figure 1. Notations

Equation (1) can be rewritten as Equation (2) using the tangential stress τ :

$$r \frac{d\sigma_r}{dr} + 2\tau = 0 \quad (2)$$

The radial deformation ϵ may be used or the distortion or shear strain γ , linked by Equation (3).

$$\gamma = 2\epsilon \quad (3)$$

Under these conditions, the specific distortion γ_c at the walls of the pressuremeter probe is linked to its current volume V and the difference since the initial state $\Delta V = V - V_0$ by Equation (4).

$$\gamma_c = \frac{\Delta V}{V} \quad (4)$$

2.1.2. Undrained conditions and small strains

Let's consider an initial volume of ground between initial radius of cavity $r_{c,0}$ and r_0 .

Initial and expanded section of the corresponding ground mass, respectively A_0 and A , are given by Equations (5) and (6)

$$A_0 = \pi(r_0^2 - r_{c,0}^2) \quad (5)$$

$$A = \pi(r^2 - r_c^2) \quad (6)$$

In undrained conditions, volumetric strain ε_v remains 0 and $A_0 = A$. In small strains, we can neglect the second order quantities, and we hence obtained the link between the distortion and the volume of the probe (length l) and the distortion level at any distance from the pressuremeter probe, as given by Equation (7) :

$$\gamma(r) = \frac{\Delta V_c}{\pi r^2 l} \quad (7)$$

2.1.3. Constitutive law

The constitutive law used for the interpretation of the test is consistent with the hyperbolic law for secant shear modulus G_{sec} given by Kondner [8] and then Hardin and Drnevich [7]: it is stated in Equation (8). Expression of tangential stress τ is then given by Equation (9).

$$\frac{G_{sec}}{G_0} = \frac{1}{1 + \frac{\gamma}{\gamma_{ref}}} \quad (8)$$

$$\tau = \frac{\gamma}{1 + \frac{\gamma}{\gamma_{ref}}} \quad (9)$$

where G_0 is the maximum value of both secant and tangent moduli. For purely cohesive soil with undrained shear strength S_u , γ_{ref} can be identified to S_u/G_0 . Equations (9) and (10) can be rewritten as (10) and (11).

$$\frac{G_{sec}}{G_0} = \frac{1}{1 + \frac{G_0 \gamma}{S_u}} \quad (10)$$

$$\tau = \frac{G_0 \gamma}{1 + \frac{G_0 \gamma}{S_u}} \quad (11)$$

Corresponding G_{sec} and τ functions of distortion γ are given in Figure 2, for $S_u/G_0 = 0,01$.

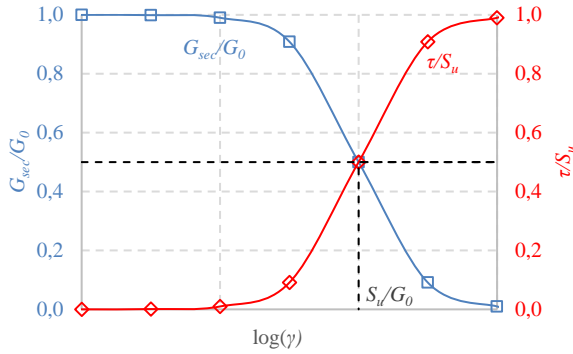


Figure 2. Secant shear modulus G_{sec} and tangential stress τ as function of distortion γ

2.3. Implementation

Equations (2), (7) and (11) can be put together to produce Equation (12):

$$\frac{d\sigma_r}{dr} + \frac{2}{r} \frac{1}{\frac{\Delta V_c G_0}{\pi r^2 l} + \frac{1}{S_u}} = 0 \quad (12)$$

As $\sigma_r = p_c$ at the cavity radius and p_0 at infinite distance of the pressuremeter probe, Equation (12) can be written successively as (13) to (17):

$$[\sigma_r]_{p_0}^{p_c} = \int_{+\infty}^r -\frac{2}{r} \frac{1}{\frac{\Delta V_c G_0}{\pi r^2 l} + \frac{1}{S_u}} dr \quad (13)$$

$$p_c - p_0 = 2 \left[\frac{S_u}{2} \left(\ln \left(\frac{\pi l}{\Delta V_c G_0} + \frac{1}{S_u r^2} \right) \right) \right]_{+\infty}^{r_c} \quad (14)$$

$$p_c - p_0 = S_u \ln \left(1 + \frac{\Delta V_c G_0}{\pi S_u r^2 l} \right) \quad (15)$$

$$p_c - p_0 = S_u \ln \left(1 + \frac{\Delta V_c G_0}{V_c S_u} \right) \quad (16)$$

$$p_c - p_0 = S_u \ln \left(1 + \gamma_c \frac{G_0}{S_u} \right) \quad (17)$$

Although based on distinct development, Equation (17) is identical to the relation given by Ferreira and Robertson [4] and provides a simple relationship between p_c , p_0 , G_0 and S_u and γ_c .

2.4. Theoretical results

2.4.1. Limit pressure

Conventional Menard limit pressure supposes the doubling of the initial volume of the probe (or $\Delta V_c/V_c = 1/2$) : under the current hypotheses, $p_{IM,HD}$ is obtained with Equation (18).

$$p_{IM,HD} = p_0 + S_u \ln \left(1 + \frac{G_0}{2S_u} \right) \quad (18)$$

Infinite volume (or strain) limit pressure $p_{l\infty,hyp}$ correspond to and infinite volume and is given by Equation (20).

$$p_{l\infty,HD} = p_0 + S_u \ln \left(1 + \frac{G_0}{S_u} \right) \quad (19)$$

These results can be compared to the same expressions as given by Gibson and Anderson [5], respectively named $p_{IM,GA}$ and $p_{l\infty,GA}$, obtained with elastoplastic constitutive law, linear elasticity and Tresca failure criterion, in Equation (20) and (21): for the following equations, G has been renamed G_{GA} to avoid any potential confusion.

$$p_{IM,GA} = p_0 + S_u \left(1 + \ln \left(\frac{G_{GA} + p_0}{2S_u} \right) \right) \quad (20)$$

$$p_{l\infty,GA} = p_0 + S_u \left(1 + \ln \left(\frac{G_{GA}}{S_u} \right) \right) \quad (21)$$

In each case, shear moduli G_0 and G_{GA} can be defined as a simple expression of p_l , p_0 , S_u . If limit pressures obtained by both methods are equals ($p_{l\infty,GA} = p_{l\infty,HD}$) and if p_0 and S_u are fixed, shear moduli G_0 and G_{GA} are linked by Equation (22) in case of considering identity of the infinite volume limit pressures :

$$G_0 = e G_{GA} - S_u \quad (22)$$

As S_u remains small compared to G_{GA} , it then appears Equation (24):

$$G_0 \approx e G_{GA} - S_u \approx 2,71 G_{GA} \quad (23)$$

Obviously a different correspondance will be obtained if conventional Menard limit pressures (and not infinite volume limit pressures) are supposed identical, as shown in Equation (24) and (25).

$$p_{IM,GA} = p_{IM,HD} \quad (24)$$

$$G_0 = e \cdot (G_{GA} + p_0) - 2S_u \quad (25)$$

2.4.2. Theoretical expansion curves

Example of theoretical p_c - γ_c , and then p_c - V_c or p_c - $\Delta r/r_0$ or (using $\gamma_c = \Delta V_c/V_c$ and $\gamma_c/2 = \varepsilon_c = \Delta r/r_c$) curves are given in Figures 3 to 5 for three sets of parameters given in Table 1 and also $V_0 = 500 \text{ cm}^3$, $p_0 = 0,2 \text{ MPa}$.

Table 1. Set of parameters for theoretical expansion curves

| n° | S_u (MPa) | G_0 (MPa) | $p_{IM,HD}$ (MPa) | $p_{l_{50},HD}$ (MPa) |
|----|----------------|----------------|----------------------|--------------------------|
| 1 | 0,2 | 20 | 0,986 | 1,123 |
| 2 | 0,2 | 40 | 1,123 | 1,261 |
| 3 | 0,1 | 20 | 0,662 | 0,730 |

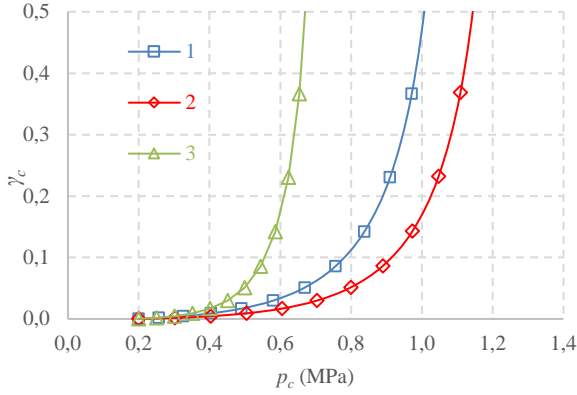


Figure 3. Theoretical p_c - γ_c curves

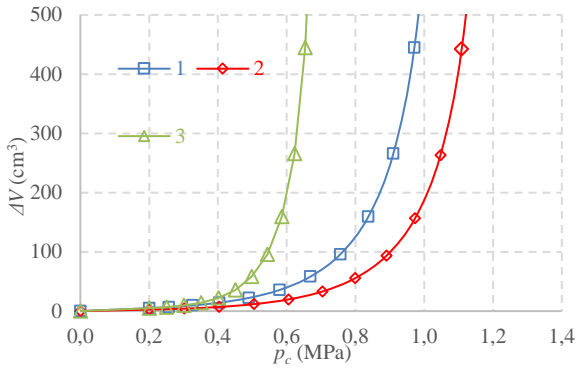


Figure 4. Theoretical p_c - ΔV_c curve

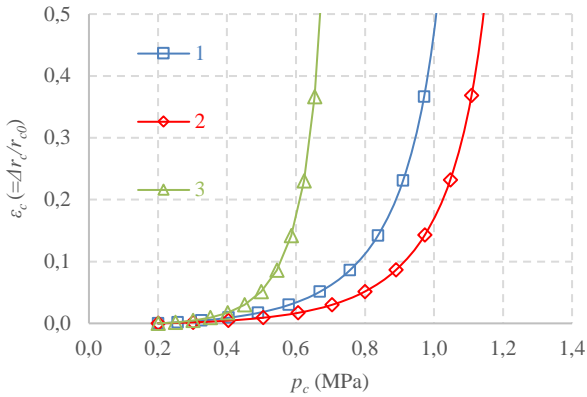


Figure 5. Theoretical p - ε_c curves1

Finally, charts can also be established to derive limit pressures from the three parameters S_u , G_0 and p_0 . An example is given for the net Menard limit pressure p_{IM}^* (where $p_{IM}^* = p_{IM} - p_0$) from S_u and the ratio G_0/S_u , on Figure 6.

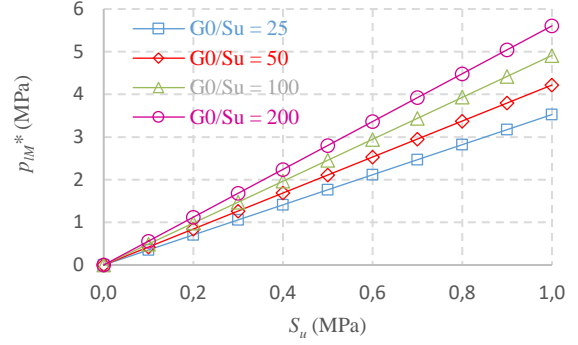


Figure 6. Theoretical p_{IM}^* values

2.4.3. Stresses in the ground

Using Equation (2), we obtained (26) :

$$\sigma_r = \alpha + \int^r -\frac{2}{r} \frac{1}{\frac{\pi r^2 l}{\Delta V_c G_0} + S_u} dr \quad (26)$$

Using the fact that $\sigma_r = p_0$ at infinite distance of the pressuremeter probe, the integration constant α can be defined that yields Equation (27) :

$$\sigma_r = p_0 + S_u \left(1 + \frac{\Delta V_c G_0}{l \pi r^2 S_u} \right) \quad (27)$$

Using again Equation (1), we can also obtain the circumferential stress, following (28) and (29) :

$$\sigma_\theta = r \frac{d\sigma_r}{dr} + \sigma_r \quad (28)$$

$$\sigma_\theta = \sigma_r - \frac{2}{\frac{\pi r^2 l}{\Delta V_c G_0} + S_u} \quad (29)$$

Evolution of theoretical radial and circumferential stresses (respectively $\sigma_{r,HD}$ and $\sigma_{\theta,HD}$) and secant modulus G_{HD} with distance to the probe is given for two ranges of applied cell pressure p_c :

- Figure 7 : $p_c = 0,3$ MPa ($p_c - p_0 \leq S_u$)
- Figure 8 : $p_c = 1$ MPa ($p_c - p_0 > S_u$)

Comparisons with solution derived from linear elasticity and elastoplasticity with linear elasticity and Tresca failure criterion are also provided, and respectively noted $\sigma_{r,GA}$ and $\sigma_{\theta,GA}$ and G_{GA} .

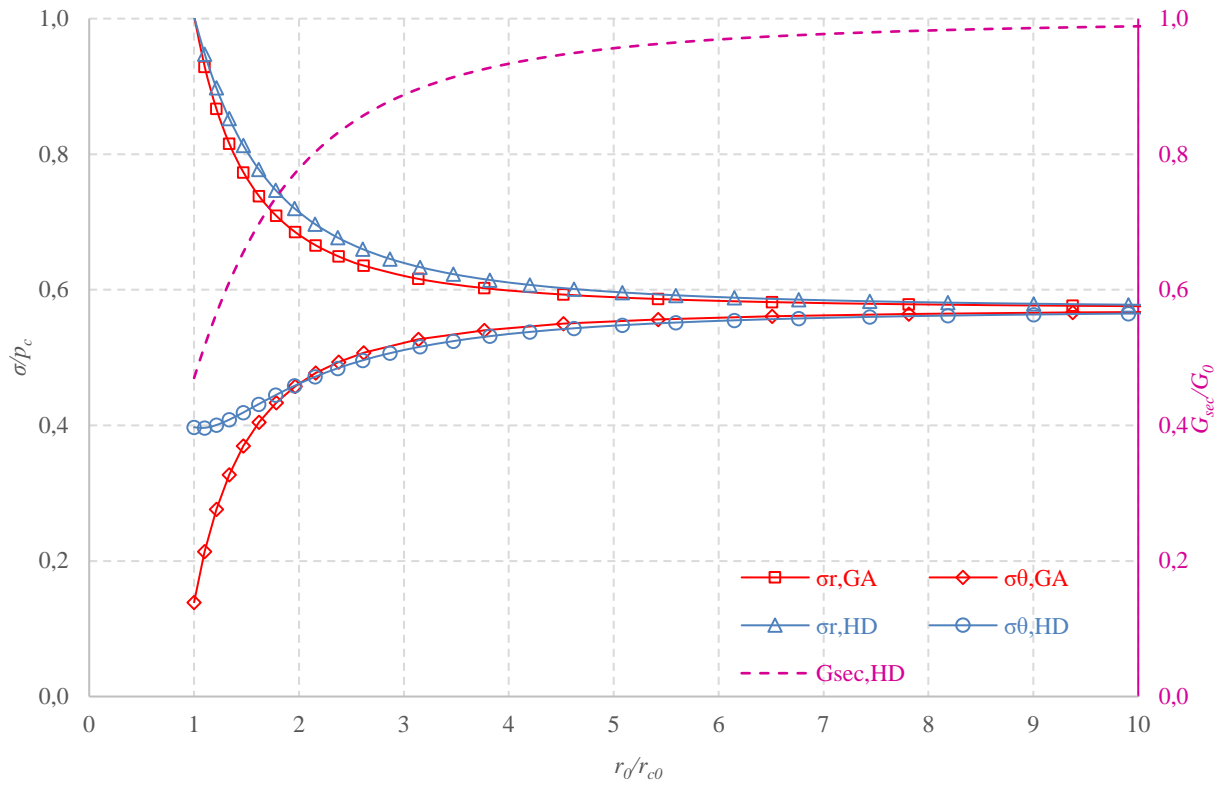


Figure 7. Stresses and shear modulus with distance to the pressuremeter probe (set of parameters 1, $p_c = 0,35$ MPa)

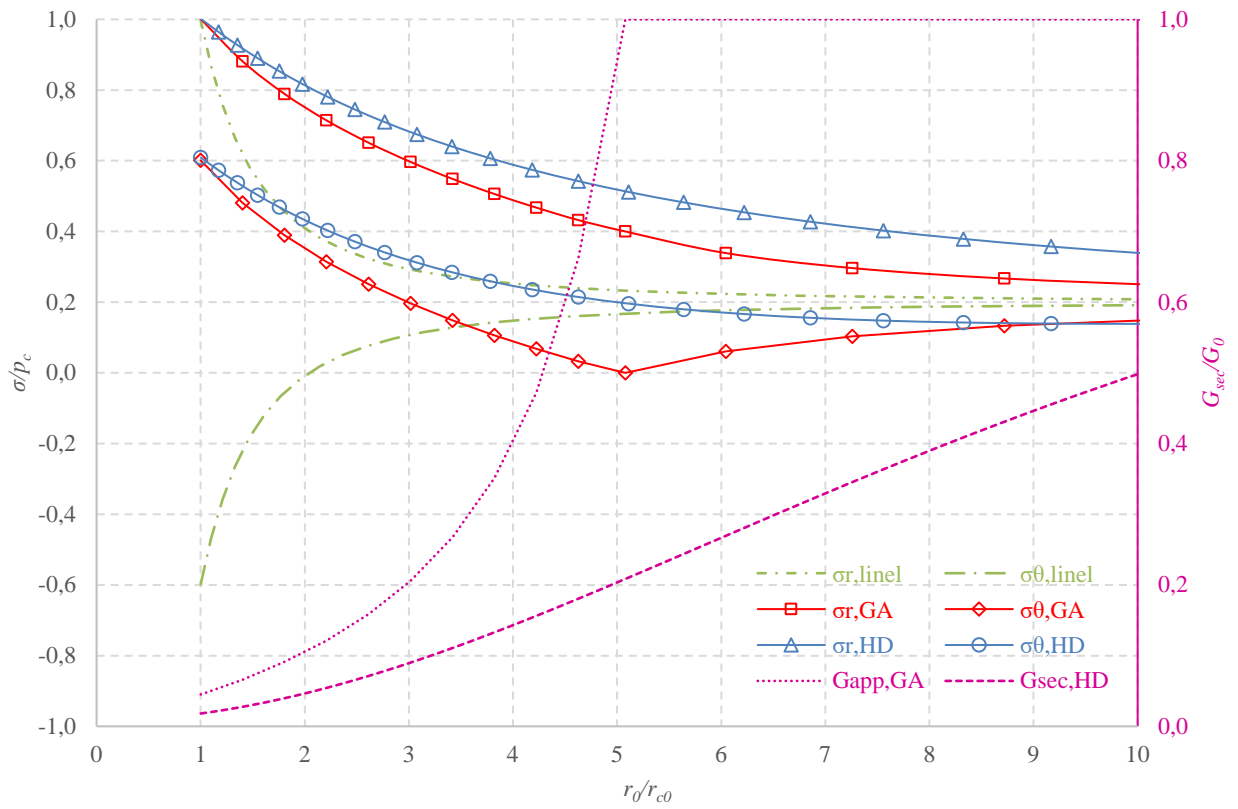


Figure 8. Stresses and modulus with distance to the pressuremeter probe (set of parameters 1, $p_c = 1$ MPa)

3. Determining shear modulus based on experimental data

3.1. Principles

Two approaches are available :

- Direct use of the p_c - V_c data,
- Overall fitting of the p_c - V_c curves.

3.1.1. Direct use of the p_c - V_c data

To determine γ - G_{sec} relationship, a first approach consists in determining $V_c \Delta p_c / \Delta V_c$, also equal to $\Delta p_c / \gamma_c$, when Δp_c and γ_c are counted after p_0 . However, as γ and subsequently G_{sec} are not homogeneous at different distances of the pressuremeter probe, this approach appears to be not relevant. Indeed Equation (20) can be used to calculate $\Delta p_c / \gamma_c$, to give Equation (31), which is clearly different from relationship (11).

$$\frac{\Delta p_c}{\gamma_c} = \frac{S_u \ln(1 + \gamma_c \frac{G_0}{S_u})}{\gamma_c} \quad (30)$$

However, we may also investigate the ratio $dp_c/d\gamma_c$. Still using Equation (19), we obtain the relationship (31).

$$\frac{dp_c}{d\gamma_c} = \frac{G_0}{1 + \frac{G_0}{S_u} \gamma_c} = \frac{1}{\frac{1}{G_0} + \frac{\gamma_c}{S_u}} = G_{sec} \quad (31)$$

Equations (20) and (32) are in fact identical: because of the non-linear elasticity of the soil around the pressuremeter probe, $dp_c/d\gamma_c$ has to be used to determine the γ_c - G_{sec} relationship. On a second step, and if necessary, knowing γ_c - G_{sec} relationship, γ - G_{tan} can also be obtained using Equation (32).

$$G_{tan} = \frac{d\tau}{d\gamma} = \frac{G_0}{(\frac{1}{\gamma G_0} + \frac{1}{S_u})^2} \quad (32)$$

In practice, if Equation (30) is unfortunately used instead of (31) to determine G_{sec} , overestimation of the shear modulus will be obtained, that can be given by Equation (33). Figure 9 shows the values obtained by each approach, and the corresponding overestimation, for different G_0/S_u ratios.

$$\Delta G_{sec} = \frac{\Delta p_c}{\Delta \gamma_c} / \frac{dp_c}{d\gamma_c} = \ln \left(1 + \gamma_c \frac{G_0}{S_u} \right) \left[\frac{S_u}{G_0} + \gamma_c \right] \quad (33)$$

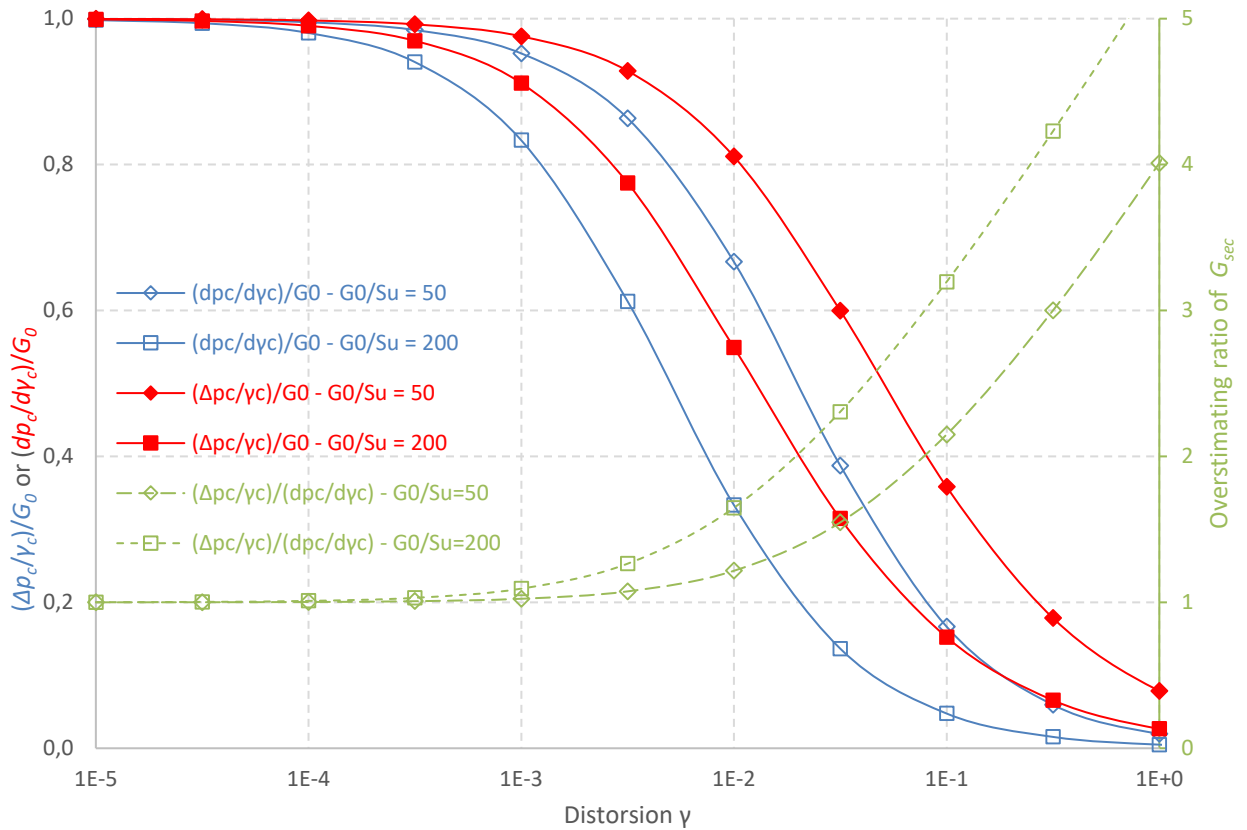


Figure 9. Overestimation of secant shear modulus

3.1.2. Fittings of the experimental curves

Different possibilities are available here, depending of the potential unloading stages performed during the pressuremeter test.

Different possibilities are then available :

- Method 1 : Direct and general fitting of the complete pressuremeter curve,
- Method 2 : Identification of S_u and $p_{l,\infty}$ or p_{IM} by the commonly accepted procedures. This

method will require an additional hypothesis for the at rest horizontal pressure p_0 ,

- Method 3 : Incorporating an unloading phase (intermediary or final) and use of the unloading phase to fit G_0 . p_0 can be then obtained to ensure consistency with $p_{l,\infty}$ or p_{IM} values.

If an unloading phase is implemented, one can use the relationship Ferreira & Robertson [4], linking the cavity

pressure p_c to the radial strain ϵ_c . Using distortion γ_c instead of radial strain ϵ_c , we then can write Equation (35) :

$$p_c = p_{c,max} + 2S_u \ln \left(\frac{1}{1 - \frac{c_0(\gamma_c - \gamma_{c,max})}{(1 + \frac{\gamma_{c,max}}{2})^2 S_u}} \right) \quad (34)$$

From a general point of view, method 1 appears difficult to implement because of the remoulding of the ground during the introduction of the pressuremeter probe in the ground, whichever the pressuremeter prebored or even selfbored. The consequences of this remoulding ground around the probe have been commonly highlighted by different authors, Baguelin et al. [1], Jefferies [10], Ferreira & Robertson [5]. They have also been studied and specifically modelled by Cambou et al. [3] and [4] for prebored pressuremeter. Consequently methods 2 and 3 will be preferred and are described below.

Undrained shear strength S_u can be identified using the slope of $dp_c/d\ln(\Delta V_c/V_c)$ ratio for the last points of the first loading phase, when ΔV_c is $V_c - V_c(p_c = p_0)$ and need an additional hypothesis on at rest earth pressure p_0 . However, as stated by Palmer (1972, [14]), the value of the undrained shear strength S_u is generally scarcely impacted by this hypothesis (Figure 11). The same approach can also be used to derive limit pressures (Table 2).

Limit pressure (and especially p_{IM} because the previous formulae are given for small strains, although solutions have also be given for large strains, Ferreira and Robertson, 1992, [6]) can be directly obtained or obtained by several available extrapolation procedures (Baguelin et al., 1978, [1]).

3.2. Application

3.2.1. Description of the pressuremeter test

The previous given procedures has been tested on a pressuremeter test in Flandres clay, in Merville, France. The test was 25 m deep and the placement of the 58 mm G-type tri-cellular probe was achieved through a preboring with a continuous flight auger. The first stage of the test was performed initially following the Menard loading procedure, but a final unloading has been added after the end of the test.

The measurement error on the volume is 1 cm^3 . The corrected pressuremeter curve is given in Figure 10, where ΔV_{60} is the injected volume after 60'' and $V_{60} - V_{30}$ the volume injected between 30 and 60''.

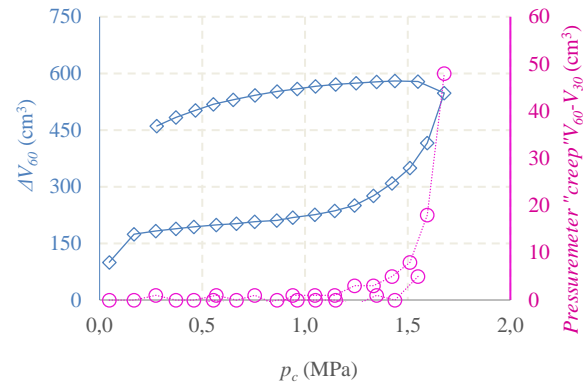


Figure 10. Experimental data

Figure 11 shows an example, with at rest earth pressure coefficient K_0 between judged "extreme" values 0,6 and 0,9, and corresponding S_u values between 307 and 327 kPa.

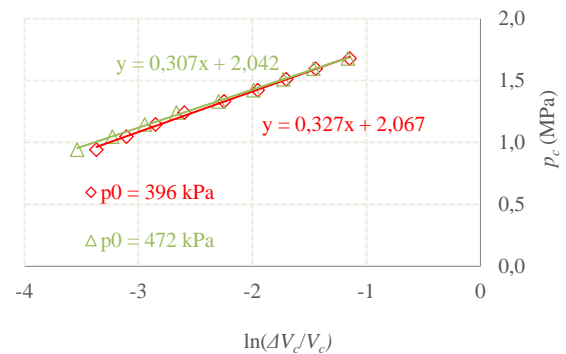


Figure 11. S_u determination

As stated before, Figure 11 also enables to extrapolate the pressuremeter curve and to determine limit pressures, For undrained conditions, taking into account the postulated linear evolution of p_c with $\ln(\Delta V_c/V_c)$. It leads to the results given in Table 2.

Table 2. Evolving of S_u and limit pressures

| p_0 (kPa) | S_u (kPa) | p_{IM} (MPa) | $p_{I\infty}$ (MPa) |
|-------------|-------------|----------------|---------------------|
| 396 | 327 | 1,840 | 2,067 |
| 472 | 307 | 1,829 | 2,042 |
| 434* | 317 | 1,834 | 2,054 |

*Best-estimate value

As stated before, Table 2 confirms that undrained shear strength S_u and limit pressures values are not sensitive to prior choice : the estimation error remains quite acceptable for engineering practice and it confirms the robustness of the chosen extrapolation.

Table 3. Standard Menard parameters

| p_{IM} (MPa) | $p_{I\infty}$ (MPa) | E_M (MPa) | G_M (MPa) |
|----------------|---------------------|-------------|-------------|
| 1,83 | 2,05 | 46,3 | 15,4 |

3.2.2. Direct use of $p_c - V_c$ data

Equation (32) is first used to obtain the secant shear modulus, directly derivating the pressuremeter $p_c - V_c$ curve (where V_c is the total volume of the cell), and the obtained results are given in Figures 12 and 13.

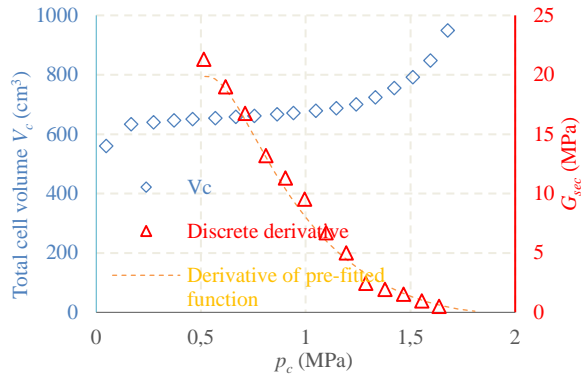


Figure 12. p_c - V_c and p_c - G_{sec} relationships

In this case, a maximum value of the secant shear modulus between 17 and 21 MPa is obtained (respectively after derivating the fitted experimental curve and).

3.3. Curve fitting or equivalent approach

3.3.1. Loading phase only

Use of loading phase requires on a first step to determine the relationships between p_0 and S_u but also p_{loc} and p_{IM} , derived from Figure 11, as shown on Figure 13.

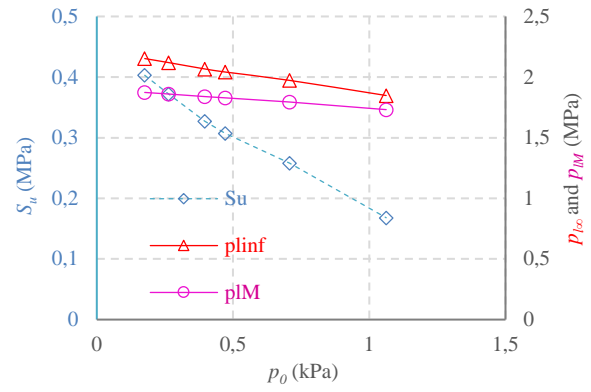


Figure 13. p_0 - S_u and p_0 - p_l relationships

On a second step, based on the probable range of the at rest earth pressure p_0 , shear modulus G_0 varying between 50 et 53 MPa is hence obtained, as shown on Figure 14.

3.3.2. Use of the unloading phase

On a second step, unloading results only are used. The use of unloading phase allows to complete Figure 15 and to obtain Figure 15. Hence, G_0 equal to 54 MPa is obtained, quite close to the one given below, although the following comments have to made :

- The mean stress does not remain constant during the loading phase, and G is likely to increase throughout the test,
- At the end of the loading phase, the vertical stress is likely to be the minimal main stress (Monnet and Chema, 1994, [12]),
- Creep effects become significant on the result (Muir Wood, [13] and Jardine, [9]).

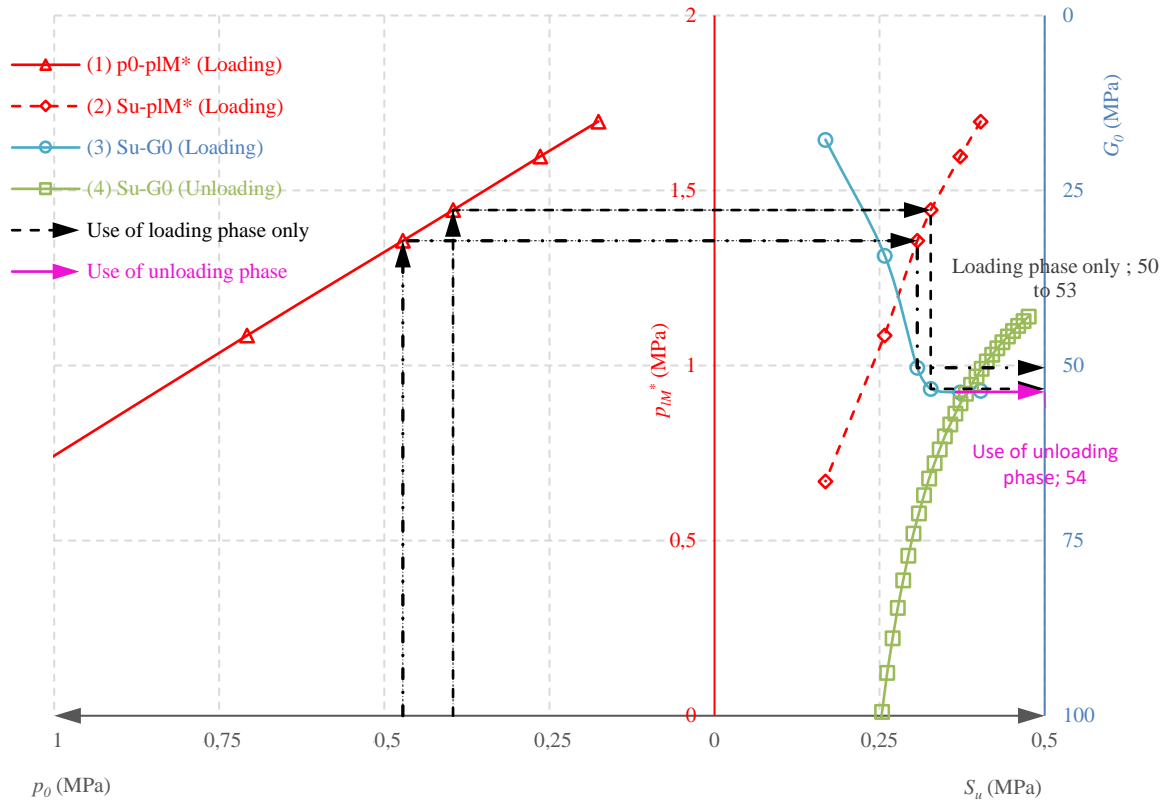


Figure 14. G_0 estimation with loading only

3.4. Synthesis

The synthesis of the shear moduli is presented in Table 4 and Figure 16 represents γ - G_{sec} relationships : the proposed method hence enables to get significant higher value of the initial shear modulus G_0 .

Table 4. G_M and G_0 values

| G_M derived from Menard modulus E_M (MPa) | | 15,4 | |
|---|--|---------------------|----------|
| G_0 (MPa) | Direct use of the pressuremeter curve (derivating) | 17 to 21 | |
| | Proposed method | Use of loading only | 51 to 53 |
| | | Use of unloading | 54 |

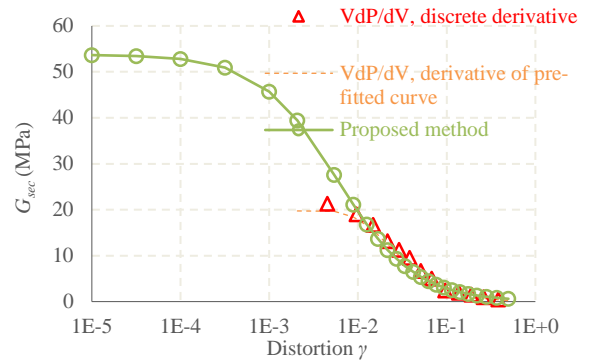


Figure 15. γ - G_{sec} relationships

Hence, it appears that implementing the proposed method may provide significantly higher values of the secant shear modulus than the one directly determined by derivating the experimental results. Both uses of loading phase only and unloading phase provide similar results.

4. Conclusion

Using a common non-linear elastic model, a pressuremeter test performed in purely cohesive soils can be interpreted to derive consistent values of the initial shear modulus and of its variation with the distortion from pressuremeter results.

Although simplified hypotheses have been used (G constant with mean stress, neglected influence of the vertical stress potentially becoming the minor main stress), use of measurements during the unloading phase during a pre-bored pressuremeter test confirm the efficiency of

the developed approach taking into account the loading phase only.

As the mean stress does not remain constant during the test, further developments could be made to assess stress-hardening behaviour of ground.

Acknowledgement

The work presented in this article has been supported by the French research project ARSCOP (new approaches of ground investigation and structures design based on pressuremeter).

References

- [1] Baguelin, F. et al., The pressuremeter and foundation engineering, Trans Tech Publications, 1978
- [2] Bolton, M.D., Whittle, R. W. , A non-linear elastic/perfectly plastic analysis for plane strain undrained expansion tests, *Geotechnique*, 49 n°1, 133-141, 1999, <https://doi.org/10.1680/geot.1999.49.1.133>
- [3] Cambou, B. et al., Determination of constitutive parameters from pressuremeter tests, 3rd International symposium of pressuremeter, London, 3, 234-253, 1990
- [4] Cambou, B. et al., Numerical analysis of pressuremeter tests : application to the identification of constitutive models, European speciality conference on numerical methods in geotechnical engineering, 368-380, 1990
- [5] Ferreira, R.S., Robertson, P. K., Interpretation of undrained self-boring pressuremeter test results incorporating unloading, *Canadian Geotechnical Journal*, 29, 918-928, 1992, <https://doi.org/10.1139/t92-103>
- [6] Ferreira, R.S., Robertson, P. K., Undrained Pressuremeter Interpretation based on loading and unloading data, *Canadian Geotechnical Journal*, 31, 71-78, 1994, <https://doi.org/10.1139/t94-008>
- [7] Gibson, R.E., Anderson, W.F., In situ measurement of soil properties with the pressuremeter, *Civil Engineering and Public Works Review*, 56, 615-618, 1961
- [8] Hardin, B.O., Drnevich, V.P., Shear modulus and damping in soils: design equations and curves, *ASCE Journal of the Soil Mechanics and Foundations Division*, 98, 1972
- [9] Jardine R., Nonlinear stiffness parameters from undrained pressuremeter tests, *Canadian Geotechnical Journal*, 29, 1992, <https://doi.org/10.1139/t92-048>
- [10] Jefferies, M.G., Determination of horizontal geostatic stress in clay with self-bored pressuremeter, *Canadian Geotechnical Journal*, 29, 1988, <https://doi.org/10.1139/t88-061>
- [11] Kondner, R.L., Hyperbolic stress-strain response: cohesive soil, *ASCE Journal of the Soil Mechanics and Foundations Division* 89, 89, 115-143, 1963
- [12] Monnet, J., Chema, T., Étude expérimentale de l'équilibre élastoplastique d'un sol cohérent autour du pressiomètre, *Revue Française de Géotechnique*, 73, 15-26, 1995
- [13] Muir Wood, D., Strain dependent moduli and pressuremeter tests, *Geotechnique*, 40, 509-512, 1990, <https://doi.org/10.1680/geot.1991.41.4.621>
- [14] Palmer, A.C., Undrained plane-strain expansion of a cylindrical cavity in clay: a simple interpretation of the pressuremeter, *Geotechnique*, 22, 451-457, 1972, <https://doi.org/10.1680/geot.1972.22.3.451>